

Simulation Study on the Vehicle Speed Control in Longitudinal Direction using a New Continuously Variable Transmission (CVT) System

Muhammad Luqman Hakim Abd Rahman
Khisbullah Hudha*
Zulkiffli Abd Kadir
Noor Hafizah Amer
Muhamad Murrad

Department of Mechanical Engineering,
Faculty of Engineering,
Universiti Pertahanan Nasional Malaysia,
Kem Sungai Besi, 57000 Kuala Lumpur, Malaysia.
*k.hudha@upnm.edu.my

ABSTRACT

In order to study the capability of Continuously Variable Transmission (CVT) system, a model of High Mobility Multipurpose Wheeled Vehicle (HMMWV) is derived and carried out in the Matlab-Simulink environment. The model consists of vehicle dynamic system, wheel dynamic system, powertrain system and tire traction system where the performance of vehicle model is compared between a stepped Automatic Transmission (AT) and CVT system equipped to the vehicle. The model is verified using CarSim results where the developed model shows a similar trend with minor deviation. A new electro-mechanical CVT system has been proposed to overcome the drawbacks of the current CVT system. Then, the developed vehicle model is implemented with vehicle speed control to study the performance of the vehicle with both transmission systems. Comparison between AT and CVT systems indicate that vehicle with CVT system shows a superior performance with higher acceleration performance and lower fuel consumption.

Keywords: Simulation; Modelling; Vehicle longitudinal dynamic; CVT system; Matlab-Simulink

Introduction

Light wheeled armoured vehicle is designed primarily for personnel and light cargo transport behind frontline during war. Upon its utilization, its capability can be boosted with a combination of tactical offensive, operational mobility and defensive capability [1]. During vehicle moving on a terrain, three types of force are exhibit on the body and wheels of a vehicle which are longitudinal forces on the x -axis, lateral forces on the y -axis, and vertical forces on the z -axis. In this case, the simulation study is focusing on the vehicle longitudinal dynamic with longitudinal and vertical forces acting on the body and wheels [2]. Since the main objective of this research is to develop a new CVT system, this paper focuses on investigating the performance of vehicle equipped with AT and CVT systems in term of acceleration and fuel consumption via simulation method.

Generally, a vehicle model is validated using an instrumented experimental vehicle which required a specialized area and a skilful driver for reducing the potential of fatal injuries and maintaining the data consistencies [3]-[4]. Another simplified approach in vehicle model validation is a model verification where the simulated model responses are compared with well-known vehicle simulation software, CarSim where it has been used as a benchmark [5]. CarSim Mechanical Simulation software is used by Original Equipment Manufacturer (OEM) as a tool for analyzing vehicle dynamic, developing an active controller, calculating vehicle performance characteristic, and engineering an active safety system. For this study, the developed vehicle model in the Matlab-Simulink environment will be verified with CarSim results by using a vehicle equipped with AT system.

CVT system is one type of automobile transmission system that offers a stepless automatic transmission with an infinite number of transmission ratio between two limits. Comparison between a vehicle equipped with a stepped AT system, vehicle with CVT system provides a smooth and continuous acceleration response resulting in lower fuel consumption and higher ride performance [6]-[7]. This study proposed a new electro-mechanical CVT system to solve current drawbacks with hydraulic-related problems and belt-misalignment phenomenon. The developed CVT system consists of two variable pulleys connected with an endless v -shaped belt by means of the contact surface between sectional pulleys and belt [8] [9]. These variable pulleys can vary the belt running radius by using electric actuators via slider-crank mechanisms. In this paper, a brief derivation of the new CVT model is presented associated with its ratio controller.

Proportional-Integral-Derivative (PID) controller is one of the most popular controllers that offers a simple control structure with high adaptability for advancing the system. It is a well-established technique for various industrial control applications due to its simple design, straightforward tuning of parameters and robust performance [10]. PID controller has been utilized in

the new CVT system where it contains feedback controls namely, motor control, radius control and ratio shift logic. Three parameters namely proportional gain, integral gain, and derivative gain need to be quantified accordingly in order to design an effective PID controller [11]. Additionally, the vehicle speed control uses PID controller to regulate the throttle input into desired vehicle speed.

This paper is divided into several sections where the first section is an introduction to the related work. The second section presents the development of vehicle longitudinal model and its component systems, followed by verification and comparison results between a simulation with CarSim model and vehicles equipped with AT and CVT systems, respectively. The last section contains the overall conclusion to this paper.

Vehicle Longitudinal Dynamic

In the simulation of vehicle dynamic performance, vehicle body and wheel dynamics are being considered where a simplified lumped body mass consists of two wheels for acceleration analysis. A schematic of vehicle dynamic presents in Figure 1 consists of a lumped mass, m which has a forward speed, V in the X -direction. The wheels of the vehicle have an angular velocity, ω_i , a wheel radius, R_i , and a moment of inertia, I_i , where $i = f, r$ represents the front and rear wheels. The distance between the front and rear axles respectively to the centre of vehicle mass are denoted by the dimension B and C , with the wheelbase denoted by the dimension L . The road inclination from the normal is indicated by the gradient, θ .

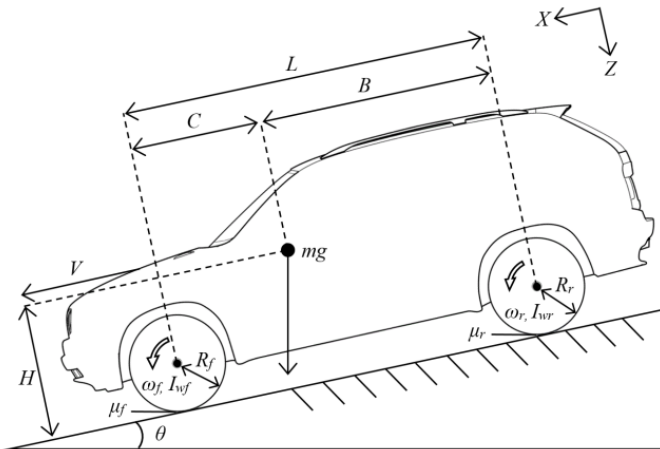


Figure 1 Schematic of vehicle dynamic in the longitudinal direction

Figure 2 shows the modelling structure of the longitudinal vehicle dynamic representing the main component of the vehicle model and the system variable dependencies among them. The main input to the model is the throttle setting and the main outputs are the vehicle, the front and rear wheel speeds. Since the purpose of this study is to investigate the performance of the transmission system, the brake input is neglected. In this modelling, wind speed and road condition are being considered due to the effect of vehicle drag force.

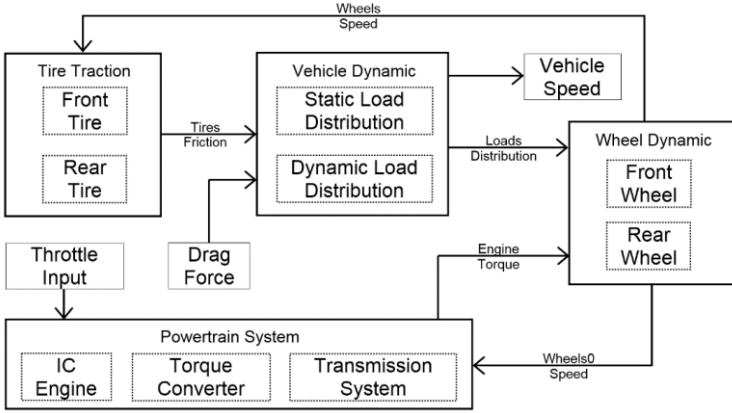


Figure 2 Longitudinal vehicle modelling structure

Vehicle forward speed V is in conjunction with the total force acting upon vehicle body, F_{X_r} , gradient road, $mg \sin(\theta)$ and drag force, F_d .

$$\dot{V} = -\frac{1}{m}(F_{X_r} - mg \sin(\theta) + F_d) \quad (1)$$

The total forces acting upon vehicle body due to normal forces, F_{Z_i} at the tire/road contact points are simply the summation of the reaction forces at the front and rear contact points.

$$F_{X_r} = 2\mu_f F_{Z_f} + 2\mu_r F_{Z_r} \quad (2)$$

The load distribution at the front and rear wheels upon vehicle body can have two terms which are static and dynamic. The static load distribution is derived from the vehicle geometry and gradient angle and then, the forces are obtained by the summation at each contact points. Meanwhile, the dynamic load distribution is governed by load transfer between the front and rear wheels

of the vehicle as it accelerates and decelerates. Thus, it is described as the front and rear normal forces.

$$F_{Z_f} = mg \left(\frac{C}{L} \cos(\theta) + \frac{H}{L} \sin(\theta) \right) - m\dot{V} \frac{H}{L} \quad (3)$$

$$F_{Z_r} = mg \left(\frac{B}{L} \cos(\theta) - \frac{H}{L} \sin(\theta) \right) + m\dot{V} \frac{H}{L} \quad (4)$$

The drag force on the vehicle can affect the vehicle performance by limiting the vehicle maximum speed due to aerodynamic and rolling resistance forces. It is affected by the frontal area of the vehicle, A , the density of air, ρ , aerodynamic drag and rolling coefficients, C_d and C_r .

$$F_d = \frac{1}{2} \rho A C_d (V^2) + mg C_r (V) \quad (5)$$

The wheel slip ratio occurs due to the difference between vehicle speed, V and rolling speed of the tire, ωR_i . A positive slip ratio indicates that vehicle exhibit greater forward speed compared to the tire rolling speed and at the extreme condition will cause tire spinning. Meanwhile, a negative slip ratio indicates that the tire exhibit greater rolling speed compared to vehicle forward speed.

$$\lambda_i = \frac{V - \omega_i R_i}{\max(V, \omega_i R_i)}, i = f, r \quad (6)$$

The tire tractive forces are the interaction of the vehicle tire and the road surface in term of friction/slip characteristics for a variety of different driving conditions and road surface. In this simulation, the Pacejka tire model is used to analyse and simulate this relationship due to its good approximation of the tire/road friction characteristic. Table 1 shows the parameters of the Pacejka tire model respectively to the road surface condition.

$$\mu_i = k_2 \sin(k_1 \tan^{-1}(k_0 \lambda_i - k_3(k_0 \lambda_i - \tan^{-1}(k_0 \lambda_i))))), i = f, r \quad (7)$$

The wheel dynamic is defined by the equivalent torque on wheels with regards to the engine torque, τ_{e_i} , the reaction torque due to the tire tractive force, $R_i F_{X_i}$, and the viscous friction torque, $\omega_i C_{f_i}$.

$$\dot{\omega}_i = \frac{1}{I_{W_i}} (\tau_{e_i} + R_i F_{X_i} - \omega_i C_{f_i}), i = f, r \quad (8)$$

Table 1 Pacejka tire parameters for different road surfaces

Surface	k_0	k_1	k_2	k_3
Dry Tarmac	10	1.9	1	0.97
Wet Tarmac	12	2.3	0.82	1
Snow	5	2	0.3	1
Ice	4	2	0.1	1

The powertrain system consists of the Internal Combustion (IC) engine, torque converter, and transmission system. In this simulation, a 150kW turbocharged diesel engine is being implemented which is represented in Figure 3. From this figure, the engine torque τ_e is functioned based on throttle setting, u_t and engine speed at the crankshaft, N_e . Optimal Operating Line (OOL) represents the characteristic of the IC engine in corresponding the CVT system requirement.

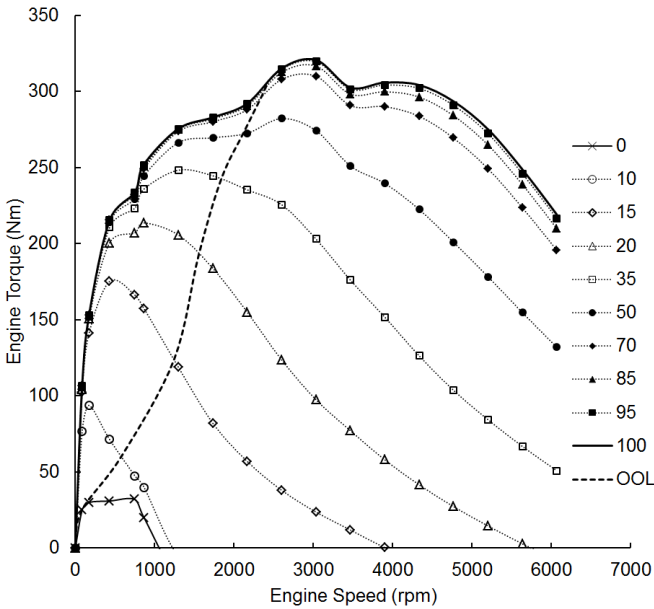


Figure 3 Engine torque characteristic respectively with throttle setting

Additionally, in the engine dynamic, vehicle fuel consumption is also analyzed in accessing vehicle performance. Figure 4 shows engine fuel rate characteristic dependently with engine speed and throttle setting.

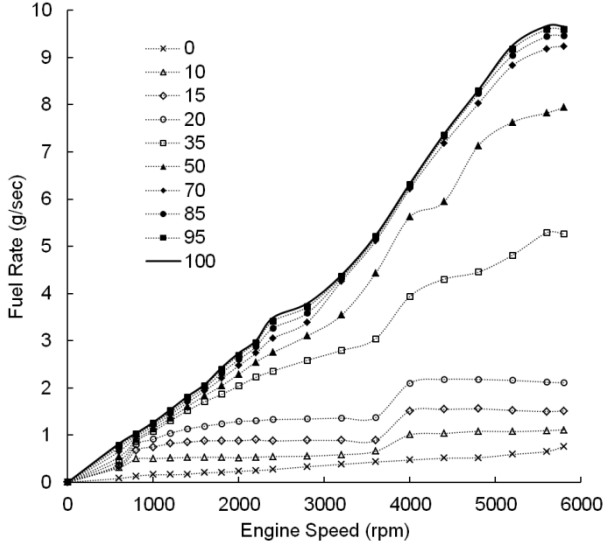


Figure 4 Engine fuel rate characteristic respectively with throttle setting

The assumption on the conversion of chemical energy into output torque by the engine is described by a first order time lag and the throttle actuation with an associated time lag, these lag can be lumped together into an equivalent lag, τ_{es} . Governing the actual amount of torque by the engine, τ_e , the wheel torque, τ_{ef} associated by the transfer coefficient, μ_e to the throttle setting, u_t is described. η_g and η_f are the current gear and final drive ratio respectively and the throttle setting is saturated in between 0-100%.

$$N_e = \eta_g \eta_f \omega_t \quad (9)$$

$$\mu_e = 0.01 u_t - \tau_{es} \dot{\mu}_e \quad (10)$$

$$\tau_{ef} = \mu_e \tau_e \eta_g \eta_f \quad (11)$$

As a part of the powertrain system, a torque converter serves as an automatic clutch for the engagement mechanism between the IC engine and transmission system. It consists of a pump connected to the output shaft of the engine, a turbine connected to the input shaft of transmission gearsets, and a stator grounded to a one-way clutch. Based on the engine dynamic, the

relationship of the torque converter can be defined in term of equivalent torque where I_e and I_p are the engine and torque converter pump moment of inertia, T_e and T_p are the torque of the engine and the torque converter pump.

$$(I_e + I_p)\dot{N}_e = T_e - T_p \quad (12)$$

The capacity factor, K and the torque ratio, TR of the torque converter are functioned of speed ratio where the speed ratio is determined from the engine speed, Ne and vehicle speed with regards to tire radius, final drive, and transmission gear ratio. Figure 5 shows the characteristic of the torque converter in term of capacity factor and torque ratio.

$$T_p = \left(\frac{N_e}{K}\right)^2 \quad (13)$$

$$T_t = T_p \cdot TR \quad (14)$$

$$SR = \frac{N_t}{N_e} \quad (15)$$

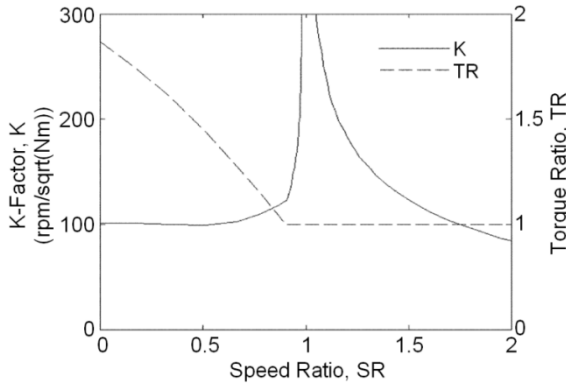


Figure 5 Characteristics of the torque converter

Automatic Transmission (AT) System

In this simulation, the Four-Wheel Drive (4WD) powertrain system is selected where IC engine in the longitudinal direction is connected to the transmission system and then assisted by the transfer case as shown in Figure 6. From the transfer case, the driving torque is distributed to the front and rear differential axles and to wheels via propeller and drive shaft. Generally, most of the

modern vehicle equipped with Automatic Transmission (AT) system are embedded to the vehicle control system where Electronic Control Unit (ECU) is monitoring many instrumented variables such as engine speed, vehicle speed, wheel speed and throttle setting. Under the various driving scenario, ECU can determine the required gear ratio for transmission based on those variables which can be described as transmission shift logic.

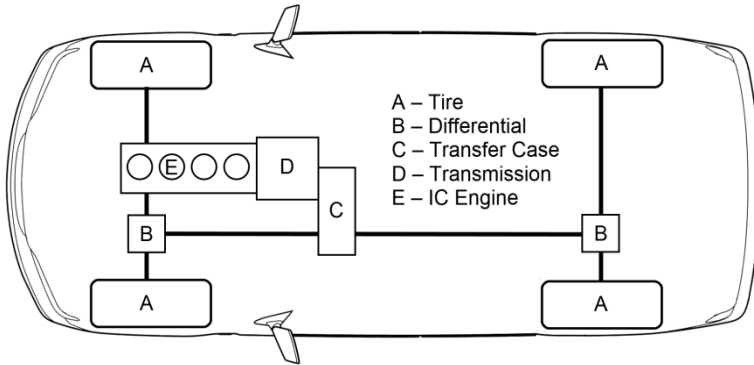


Figure 6 Configuration of the four-wheel drive powertrain system

The transmission shift logic is related to the threshold for changing the designated gear up and down as a function of throttle setting and wheel speed. From Figure 7, there are two corner points in the shift profile of each designated gear correspond to the throttle setting at 20% and 80% respectively. This allows the engine to operate at the desired region of its torque curve most of the time.

Continuously Variable Transmission (CVT) System

In modelling CVT system, the Optimum Operating Line (OOL) serves as the main component for determining the required transmission ratio for IC engine. In order to determine the OOL line, the linear approximated locus of optimum operating points is used as in Equation (16), where N_r and T_r are the engine rated speed and torque [12]. Through this method, a suitable OOL is determining based on the engine characteristic. Given the engine has a rated torque and speed of 320 Nm at 3033 rpm, by using equation (16), the engine speed, N_o and torque, T_o of OOL profile points, can be described as in Table 2. From Figure 8, OOL logic will determine the required CVT ratio based on torque and speed of the engine dependently to throttle input and vehicle speed as a function of wheel speed.

$$\left(\frac{N}{N_r}\right) = 0.86\left(\frac{T}{T_r}\right) - 0.06 \quad (16)$$

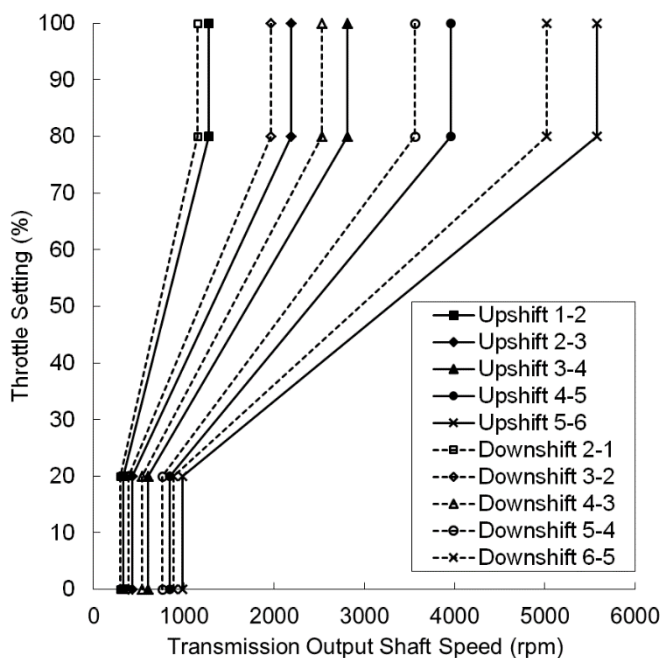


Figure 7 6-speed automatic transmission shift logic

Table 2 Optimal operating point for the 150 kW turbocharged diesel engine.

Throttle Input (%)	Specific Maximum Torque (Nm)	Optimal Engine Speed (rpm)	Optimal Engine Torque (Nm)
0	32	78	24
10	93	580	60
15	175	1244	123
20	213	1556	192
35	248	1838	242
50	282	2113	272
70	310	2339	296
85	316	2394	302
95	319	2418	305
100	320	2426	305

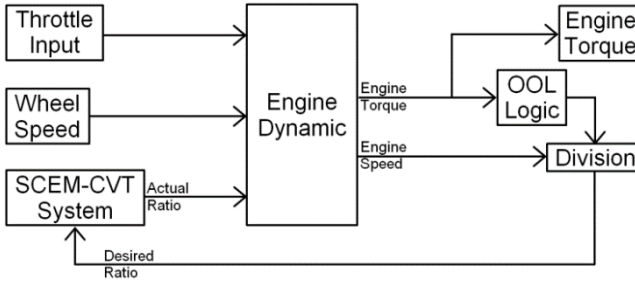


Figure 8 CVT system configuration

CVT system used in this vehicle modeling consists of two variable pulley connected with an endless v-belt having various transmission ratio as shown in Figure 9. The variable pulley consists of a slider-crank mechanism which is actuated by a DC motor through a power screw mechanism as shown in Figure 10 [8]. The CVT variable pulley is represented dynamically using Lagrange formulation as in Equation (17) - (20) where the pivot, the length and the centre of arm 1 are denoted as point o , l_1 and c_1 , respectively. Meanwhile, the length and centre of the arm 2 are denoted as l_2 and c_2 respectively. Then, the length and the height of slider 3 are denoted as l_3 and l_6 respectively. For arm 4, its length and centre are denoted as l_4 and c_4 respectively. Last, the length and the height of slider 5 are denoted as l_5 and l_7 respectively. The angle of θ_1 , θ_2 and θ_3 are denoted as the angle between arm 1, arm 2 and arm 4 respectively with the x -axis, while the displacement of the sectional pulley is denoted by y . All the simulation parameters for CVT driver and driven pulleys are listed in

Table 4 and
Table 5.

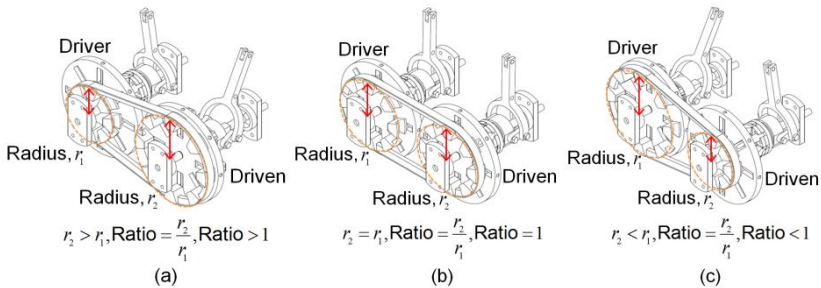


Figure 9 A new CVT mechanism with slider crank mechanism where (a) ratio bigger than 1, (b) ratio equal to 1, and (c) ratio of less than 1

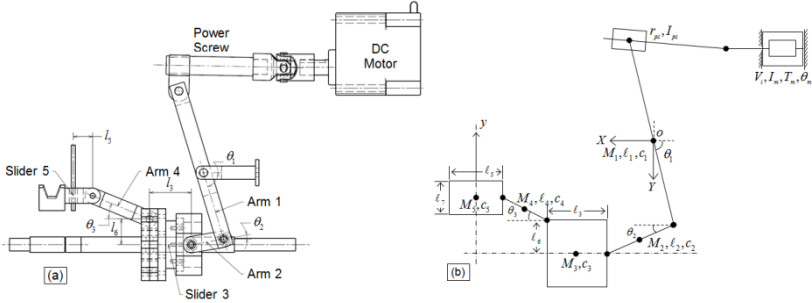


Figure 10 (a) Schematic and (b) free body diagrams of CVT variable pulley.

$$\left(I_1 + (M_2 + M_4 + M_5) \ell_1^2 \right) \ddot{\theta}_1 + \left(\frac{1}{4} M_2 + M_4 + M_5 \right) \ell_1 \ell_2 \ddot{\theta}_2 - \left(\frac{1}{2} M_4 + M_5 \right) \ell_1 \ell_4 \ddot{\theta}_3 + \left(\frac{1}{2} M_1 + M_2 + M_3 + M_4 + M_5 \right) g \ell_1 = T \quad (17)$$

$$\left(I_2 + \left(\frac{1}{4} M_2 + M_4 + M_5 \right) \ell_2^2 \right) \ddot{\theta}_2 + \left(\frac{1}{4} M_2 + M_4 + M_5 \right) \ell_1 \ell_2 \ddot{\theta}_1 - \left(\frac{1}{2} M_4 + M_5 \right) \ddot{\theta}_3 + \left(\frac{1}{2} M_2 + M_3 + M_4 - M_5 \right) g \ell_2 = 0 \quad (18)$$

$$\left(I_4 + \frac{1}{4} M_4 \ell_4^2 + M_5 \ell_4^2 \right) \ddot{\theta}_3 - \left(\frac{1}{2} M_4 + M_5 \right) \ell_1 \ell_4 \ddot{\theta}_1 - \left(\frac{1}{2} M_4 + M_5 \right) \ell_2 \ell_4 \ddot{\theta}_2 - \left(\frac{1}{2} M_4 + M_5 \right) g \ell_4 = 0 \quad (19)$$

$$y = \ell_1 \theta_1 + \ell_2 \theta_2 - \frac{1}{2} \ell_6 - \ell_4 \theta_3 \quad (20)$$

Figure 11 shows the structure of the CVT ratio controller consists of two separate feedback control systems for the driver and driven sectional pulleys for incorporating with the ratio shift logic scheme. Each of the feedback control systems contains two controller feedback loops in delivering the desired radial position of the sectional pulley, namely radius control and position tracking control for DC motor. Based on the desired ratio, pulley radius controller then determines the radius position of the sectional pulley, which will then be the input for position tracking controller that will regulate

the speed and torque from DC motor in delivering the desired radial position of the variable pulley inefficient manner.

Referring to the transmission ratio in the automatic transmission, the CVT ratio is suited together between 0.61 up to 3.10.

Figure 12 shows the designated CVT ratio as a function to the driver and driven pulley, respectively. The driver pulley can vary its radius from 25.0mm up to 72.0mm, while the driven pulley can vary its radius from 44.0mm up to 77.5mm.

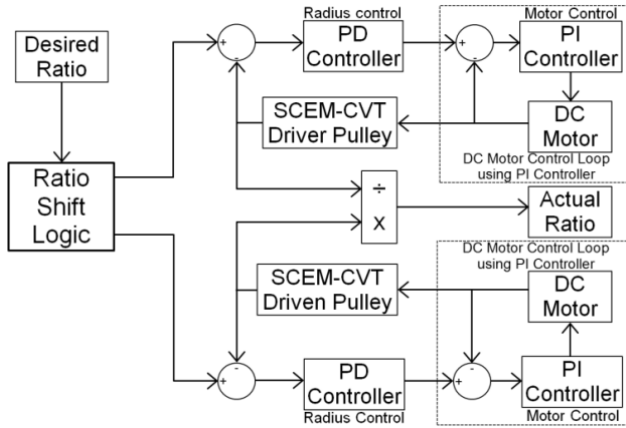


Figure 11 Control structure of the CVT mechanism

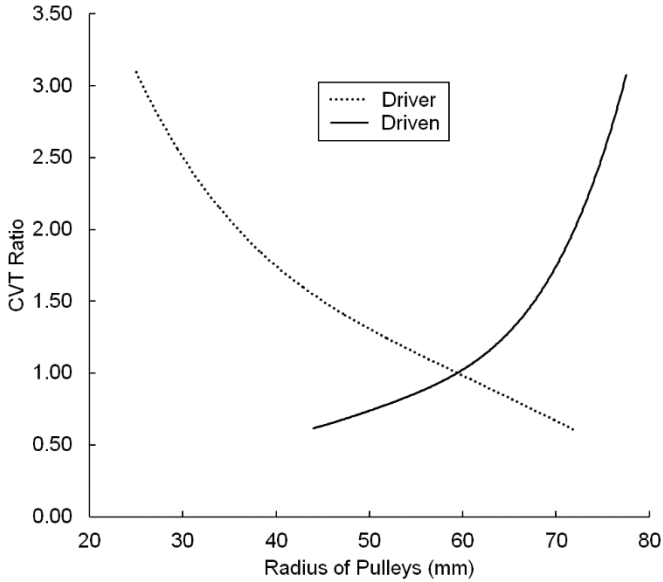


Figure 12 CVT ratio respectively with the driver and driven pulley radius positions

Vehicle Model Verification

Throughout this section, the overall parameters of vehicle modelling are presented with vehicle model verification results. The vehicle selected for this purpose of this study is High Mobility Multipurpose Wheeled Vehicle (HMMWV) with a 150 kW turbocharged diesel engine and 6-speed automatic transmission which can be assessed from the CarSim software. Table 3 shows the overall parameters required in order to simulate the HMMWV dynamic model and its transmission profile.

Table 4 to Table 6 show the parameters of CVT driver and the driven pulley and its controller, respectively where the parameters are obtained from Computer Aided Design (CAD) software.

Table 3 Parameters of HMMWV model

Wheelbase, L	3.302m
Distance front axle from vehicle centre of gravity, C	1.070m
Distance rear axle from vehicle centre of gravity, B	2.232m
Height of vehicle centre of gravity, H	0.660m

Wheel radius, R_i	0.465m
Wheel rotational inertia, I_{w_i}	4.5kgm ²
Gravitational acceleration, g	9.81ms ⁻²
Air density, ρ	1.23kg/m ³
Aerodynamic drag coefficient, C_d	0.29
Rolling resistance coefficient, C_r	0.01
Viscous friction coefficient, C_{f_i}	0.10Nm/rads ⁻¹
Equivalent lag, τ_{es}	0.01s
Crankshaft rotational inertia, I_e	0.200kgm ²
Torque converter pump rotational inertia, I_p	0.015kgm ²
Final gear ratio, η_f	4.10
First gear ratio, η_1	3.10
Second gear ratio, η_2	1.81
Third gear ratio, η_3	1.41
Fourth gear ratio, η_4	1.00
Fifth gear ratio, η_5	0.71
Sixth gear ratio, η_6	0.61

Table 4 Parameters of CVT driver pulley model

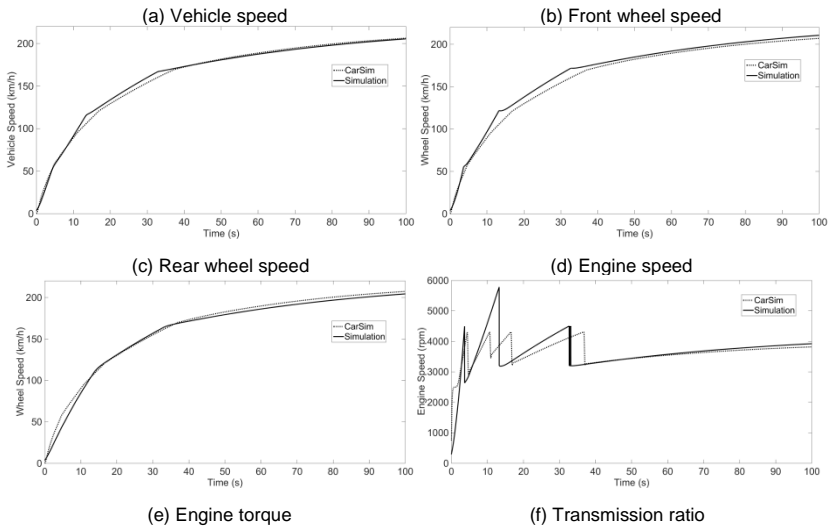
Parts	Mass (kg)	Moment of Inertia (kgm ²)	Length (m)
Arm 1 (fork arm)	$M_1 = 0.40$	$I_1 = 7.51 \times 10^{-4}$	$\ell_1 = 0.07$
Arm 2 (fork bracket)	$M_2 = 0.05$	$I_2 = 9.10 \times 10^{-6}$	$\ell_2 = 0.03$
Slider 3 (pusher bearing and arm carrier)	$M_3 = 0.62$		$\ell_3 = 0.04$ $\ell_6 = 0.02$
Arm 4 (slider arm)	$M_4 = 0.11$	$I_4 = 3.06 \times 10^{-5}$	$\ell_4 = 0.07$
Slider 5 (sectional pulley)	$M_5 = 0.13$		$\ell_5 = 0.04$ $\ell_7 = 0.02$

Table 5 Parameters of CVT driven pulley model.

Parts	Mass (kg)	Moment of Inertia (kgm ²)	Length (m)
Arm 1 (fork arm)	$M_1 = 0.40$	$I_1 = 7.51 \times 10^{-4}$	$\ell_1 = 0.07$
Arm 2 (fork bracket)	$M_2 = 0.05$	$I_2 = 9.10 \times 10^{-6}$	$\ell_2 = 0.03$
Slider 3 (pusher bearing and arm carrier)	$M_3 = 0.82$		$\ell_3 = 0.04$ $\ell_6 = 0.04$
Arm 4 (slider arm)	$M_4 = 0.10$	$I_4 = 2.86 \times 10^{-5}$	$\ell_4 = 0.06$
Slider 5 (sectional pulley)	$M_5 = 0.13$		$\ell_5 = 0.04$ $\ell_7 = 0.02$

Table 6 Parameters of the radius controller for CVT pulleys

Parameter	Motor controller	Radius controller
Proportional gain, K_p	50	150
Integral gain, K_i	175	0
Derivative gain, K_d	0	1



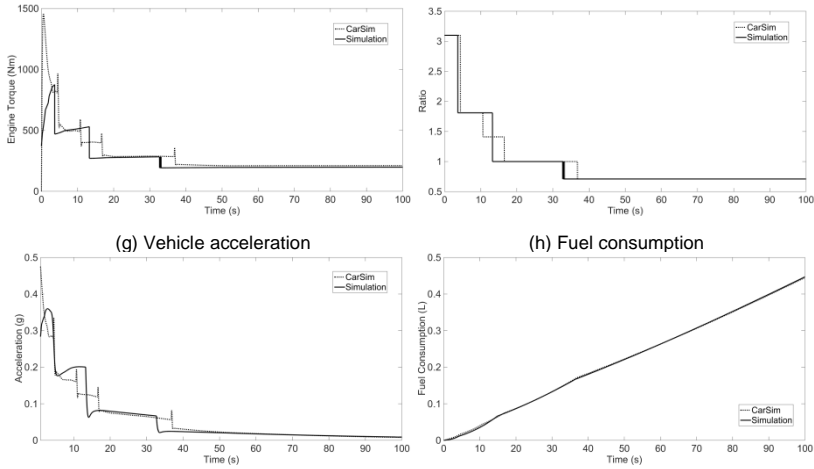


Figure 13 Comparison of vehicle dynamic response between CarSim and simulation results.

The longitudinal vehicle dynamic model is simulated in a MATLAB-SIMULINK environment where the vehicle is assumed to be driven on a flat dry tarmac road surface. In order to verify the simulation model, the full throttle test is selected where the simulation study is performed for a period of 100 seconds using Bogacki-Shampine solver with a fixed step size of 0.01 second. A series of vehicle response is compared between CarSim software and simulation model which is vehicle speed, front and rear wheel speed, engine speed and torque, transmission ratio, vehicle acceleration and fuel consumption. Figure 13 shows the response comparison between CarSim software and simulation model. From those responses, it can be concluded that the simulation model is adequately suitable in following the behaviour of HMMWV model, although there is slight deviation occur in the powertrain response. It is due to the fact that CarSim software consists of the higher order of multi-body dynamic and kinematic.

Vehicle Speed Control

Vehicle speed control normally comprises the throttle input function in maintaining the vehicle desired speed which is shown in Figure 14. In this study, the vehicle speed control is being implemented into both vehicles equip with AT and CVT systems. The response of vehicle with AT system will be used as a benchmark for studying the capability of the vehicle with CVT system. It is assumed that both vehicles are equipped with Electronic Throttle Body (ETB) where the throttle can be controlled electronically in following the desired vehicle speed. A Proportional-Integral-Derivative (PID) controller

is selected for this study due to its simple and robust structure in adapting to another advance controller. Table 7 shows the parameters for the vehicle speed controller. A combination of acceleration and deceleration tests is being simulated to study the capability of the vehicle with CVT system compared to a vehicle with AT system. The simulation test is carried out where the vehicle is set to accelerate at around 90km/h then decelerate and maintain at 60km/h.

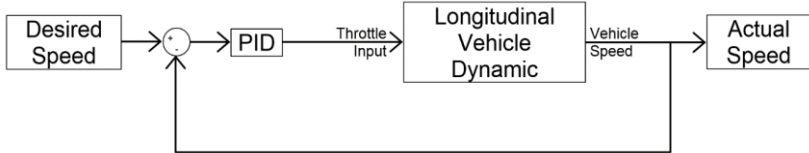
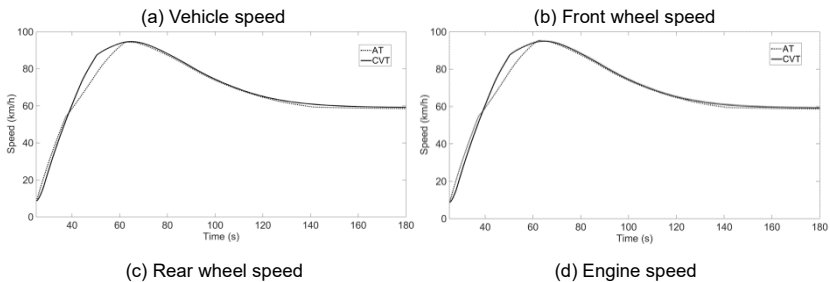


Figure 14 Structure of vehicle speed controller

Table 7 Parameters of vehicle speed controller

Proportional gain, K_p	25
Integral gain, K_i	0.5
Derivative gain, K_d	0

Figure 15 presents the comparison of the vehicle with AT and CVT systems comprise vehicle speed controller with a combination of acceleration and deceleration tests. The vehicle and wheel speeds responses show that during initial speed (0-60 km/h), a vehicle with CVT is slightly behind around 2 seconds until the period of 40 seconds. Due to transmission shifting event of the vehicle with AT at 40 seconds, it experiences a speed drop where the acceleration of vehicle drop instantaneously before gaining it back, while a vehicle with CVT keeps gaining more speeds constantly due to the smooth transition of the transmission ratio.



Simulation Study on the Vehicle Speed Control using a New CVT System

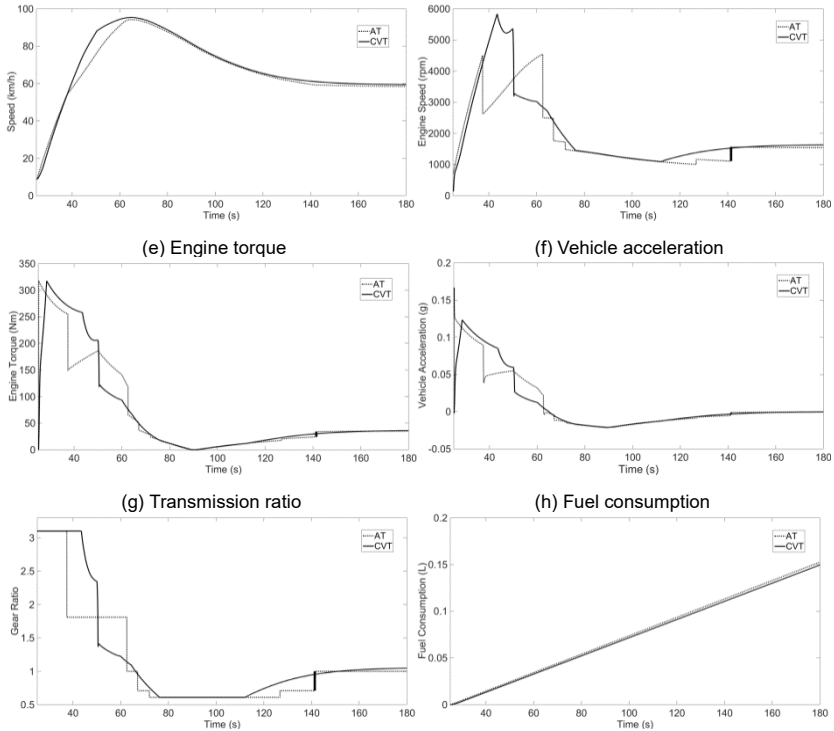


Figure 15 Comparison of vehicle dynamic response upon the implementation of a vehicle speed control system between a vehicle with AT and CVT systems.

Comparison in term of speed and torque of the engine, it shows that vehicle with CVT can maintain more its speed and torque during the transition of transmission ratio which provides a smooth acceleration while retaining its optimum operating condition. However, a vehicle with CVT experiences higher engine speed during accelerates and lower engine speed during deceleration by comparison between a vehicle with AT. In term of vehicle acceleration and transmission ratio, a vehicle with CVT shows a superior performance where it experiences smooth driving forces due to an infinite number of transmission ratio which could not happen in a vehicle with AT due to discrete transmission ratio. In term of fuel consumption, a vehicle with CVT utilizes 5% lesser fuel compared with a vehicle with AT due to it can maintain its engine optimum condition more without disruption by shifting gear of transmission system.

Conclusion

Simulation study on modelling of vehicle longitudinal dynamic had been carried out successfully in the Matlab-Simulink environment. Upon verification, simulation model could adequately follow the trend of CarSim software, although slight deviations occurred in the powertrain system, yet the simulation model responses still acceptable. Then, a new type of CVT system was introduced which could solve drawbacks in current CVT system. Through implementation on vehicle speed control, the vehicle with CVT system showed promising results in term of acceleration and fuel consumption. Future works on this study would focus on Hardware-in-the-Loop-Simulation (HiLS) implementation and multi-objective system on vehicle speed controller in improving further the application of the CVT system.

Acknowledgements

This work is part of the research project entitled Robust Stabilization of Armored Vehicle Firing Dynamic Using Active Front Wheel Steering System. This research is fully supported by LRGS grant (No. LRGS/B-U/2013/UPNM/DEFENSE & SECURITY – P1) lead by Assoc. Prof. Dr Khisbullah Hudha. The authors would like to thank the Malaysian Ministry of Science, Technology and Innovation (MOSTI) and Universiti Pertahanan Nasional Malaysia (UPNM) for their continuous support in the research work.

References

- [1] S. J. Zaloga, “HMMWV Humvee 1980–2005: US Army tactical vehicle”, Bloomsbury Publishing (2011).
- [2] M. Short, M. J. Pont and Q. Huang, “Simulation of vehicle longitudinal dynamics”, *Safety and Reliability of Distributed Embedded Systems*, 04-01 (2004).
- [3] F. Ahmad, K. Hudha and M. H. Harun, “Pneumatically actuated active suspension system for reducing vehicle dive and squat”, *Jurnal Mekanikal*, (28), 85-114 (2009).
- [4] K. Hudha, Z. A. Kadir and H. Jamaluddin, “Simulation and experimental evaluations on the performance of pneumatically actuated active roll control suspension system for improving vehicle lateral dynamics performance”, *International Journal of Vehicle Design*, 64(1), 72-100 (2014).
- [5] M. I. Satar, K. Hudha, W. A. W. Mat, R. N. I. R. Othman, M. Murrad, V. R. Aparow and M. S. Salleh, “Modelling and verification of 5 degree of freedom vehicle longitudinal model”, In 10th Asian Control Conference (ASCC), 2015, (pp. 1-6), IEEE Transaction (2015).
- [6] W. D. Dunham, J. Seok, W. Chen, E. Dai, I. Kolmanovsky and A. Girard, “Control of Gear Ratio and Slip in Continuously Variable Transmissions:

- A Model Predictive Control Approach”, SAE Technical Paper (No. 2017-01-1104) (2017).
- [7] T. Kudo, Y. Moriyoshi, T. Kuboyama, T. Yamada, K. I. Koseki and Y. Akiyama, “Driving Cycle Simulation of a Vehicle with Gasoline Homogeneous Charge Compression Ignition Engine Using a Low-RON Fuel”, SAE Technical Paper (No. 2016-01-2297) (2016).
 - [8] I. I. Mazali, K. B. Tawi, B. Supriyo, N. A. Husain, M. S. C. Kob and M. S. C. Kob, “Transmission ratio calibration for electro-mechanically actuated continuously variable transmission”, *International Journal of Advanced Mechatronic Systems*, 7(3), 127-133 (2017).
 - [9] M. L. H. Abd Rahman, K. Hudha, Z. A. Kadir, N. H. Amer, and V. R. Aparow, “Modeling and Validation of a Novel Continuously Variable Transmission using Slider Crank Mechanism”. *International Journal of Engineering Systems Modelling and Simulation (IJESMS)*, 10(1), 49-61, (2018). In Press
 - [10] H. S. M. Bakheat, A. O. A. Yaqoub and A. K. A. Elzoher, “Proportional-Integral-Derivative (PID) for Speed Control of DC Motor”, Doctoral Dissertation, Sudan University of Science and Technology (2016).
 - [11] M. A. A. Algdal, M. A. M. Altaher, M. A. AbdElkareem and A. A. AbdElrhman, “Studying The Theory of PID Controller & Comparing Its Tuning Methods”, Doctoral Dissertation, Sudan University of Science and Technology (2016).
 - [12] M. Gonzalez-de-Soto, L. Emmi, I. Garcia and P. Gonzalez-de-Santos, “Reducing fuel consumption in weed and pest control using robotic tractors”, *Computers and Electronics in Agriculture*, 114, 96-113 (2015).